On the Dynamic Dielectric Behaviour of $(CH_3NH_3)_3Sb_2Br_9$(MABA)

Czesław Pawlaczyk and Ryszard Jakubas[a]

Institute of Molecular Physics, Polish Academy of Sciences,
Smoluchowskiego 17, 60-179 Poznań, Poland
[a] Faculty of Chemistry, University of Wrocław, F. Joliot-Curie 14, 50 383 Wrocław, Poland

Reprint requests to Prof. R. J.: Fax: +48 71 328 2348; E-mail; rj@wchuwr.chem.uni.wroc.pl

Z. Naturforsch. **58a,** 189 – 193 (2003); received December 2, 2002

The complex electric permittivity of ferroelectric $(CH_3NH_3)_3Sb_2Br_9$ (MABA) single crystals has been measured in the frequency range 1 kHz – 3 GHz between 15 and 300 K. The dynamic dielectric behaviour of MABA is determined by the properties of high frequency relaxation of Cole-Cole type. It is thermally activated and characterised by a relatively small activation energy. The phase transitions at 168 and 134 K influence the amplitude of the relaxation ($\Delta\varepsilon$) without any important changes in the relaxation frequency.

Key words: Dielectric Response; Phase Transitions; Ferroelectrics.

1. Introduction

The alkylammonium halogenoantimonates(III) and bismuthates(III) crystals of the general formula $R_aM_bX_{3b+a}$ (R = organic cation, M = Sb or Bi, X = Cl, Br, I) form various structures, mainly with an anionic sublattice built by MX_6 octahedra sharing corners, edges or faces [1 – 2]. Special attention attracts the $R_3M_2X_9$ subclass of crystals because of their interesting ferroic properties. Several crystals having such stoichiometry exhibit ferroelasticity and ferroelectricity [3 – 10]. It has turned out that ferroelectric properties appear only for crystals having two-dimensional layers of polyanionic $M_2X_9^{3-}$ units. The structural phase transitions found in these crystals are governed by the ordering of organic cations. $(CH_3NH_3)_3Sb_2Br_9$ (MABA) crystallizes at room temperature with trigonal symmetry (space group $P\bar{3}ml$), similarly as its bismuth analogue $(CH_3NH_3)_3Bi_2Br_9$ (MABB) [11, 12]. In spite of the fact that both methylammonium crystals are isomorphous at room temperature, they reveale a different sequence of phase transitions:

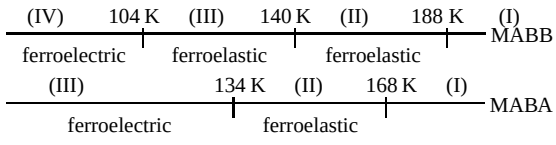

The polar phase (III) of MABA is characterised by quite small spontaneous polarization of the order of $1.5 \cdot 10^{-3}$ C·m^{-2} along the a-axis of the trigonal phase (I). Brillouin studies showed that the phase transition at 168 K is driven by an order-disorder relaxation mode (C_{66}) and is induced at the Γ-point of the room temperature phase [13].

The motional state of the methylammonium cations in different phases of MABA has been determined recently by means of ^{1}H and ^{2}D NMR measurements [14]. The high temperature phase (I) is characterized by isotropic rotation of two different types of methylammonium cations. The I→II phase transition is connected with the onset of freezing off the motion along the C–N axis of all methylammonium cations (three types). Over the intermediate phase (II), during cooling, the freedom of motions of methylammonium cations is continuously diminished. Just below the II→III phase transition the C–N axis is fixed, whereas the C_3 type of motion of NH_3 and CH_3 groups still takes place. The change in the dynamical state of the methylammonium cations is also reflected by the dielectric response of this crystal. The freezing of the rotational motion of the cations in the C-N axis at 168 and 134 K leads to a step-wise decrease of the electric permittivity when the phase transition is crossed [12].

In this paper the properties of the high frequency contribution of the dielectric relaxation (up to 3 GHz) in the vicinity of the 168 and 134 K phase transitions of MABA crystals are presented. The mechanism of the phase transitions is discussed.

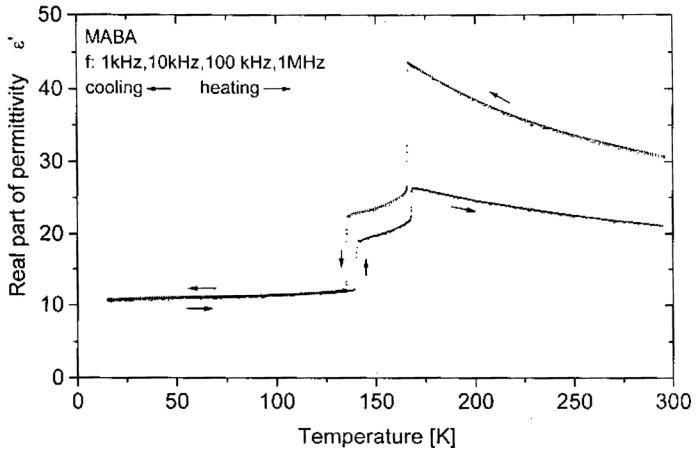

Fig. 1. Temperature dependence of the low frequency electric permittivity (ε') in the temperature range from 15 to 300 K for the frequencies between 1 kHz and 1 MHz along the *c*-axis of MABA crystal.

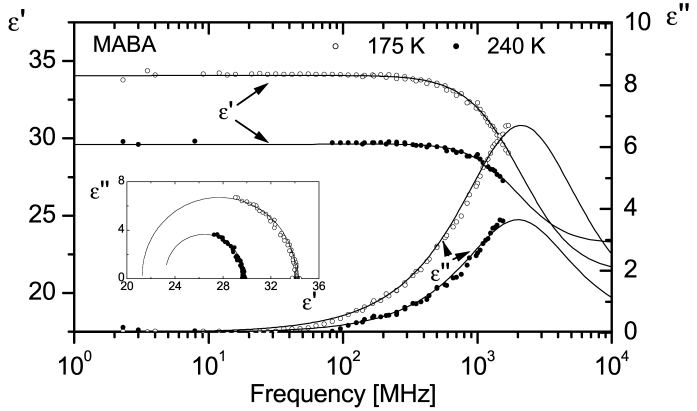

Fig. 2. Frequency dependence of ε' and ε'' and Cole-Cole plots (insert) for MABA crystal in the paraelastic phase (I) at 240 and 175 K.

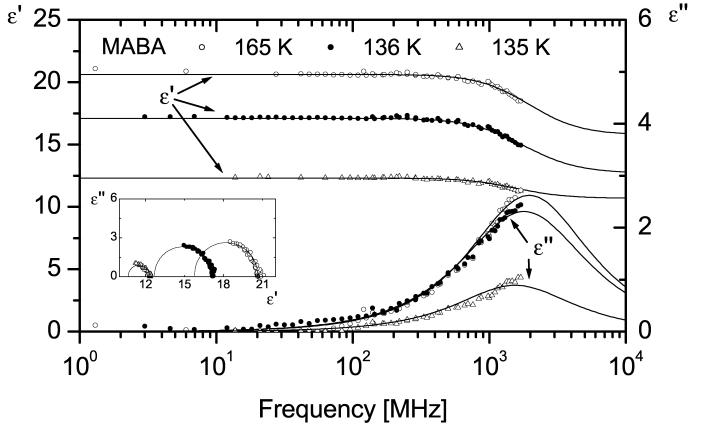

Fig. 3. Frequency dependence of ε' and ε'' and Cole-Cole plots (insert) for MABA crystal in the ferroelastic phase (II) at 165, 136 and 135 K.

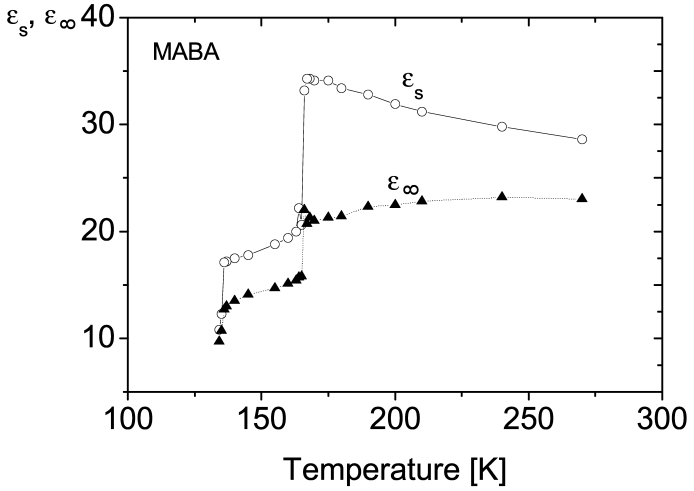

Fig. 4. Temperature dependence of the high and low frequency limiting values of the electric permittivity, ε_s and ε_∞, respectively.

2. Experimental

Single crystals of $(CH_3NH_3)_3Sb_2Br_9$ (MABA) were grown by slow evaporation of an aqueous solution containing 3:2 mole fractions of CH_3NH_2 and $SbBr_3$ with concentrated HBr. Yellow and transparent crystals in the form of hexagonal plates were obtained.

The dielectric measurements were done on discs of 2–4 mm diameter and 0.5–1 mm thickness with the symmetry axis of the disc parallel to the *c* axis of the MABA crystal. Dielectric measurements in the frequency range 100 Hz–1 MHz were done using an HP 4575A LCR meter. In the frequency range 1 MHz–3 GHz the complex dielectric permittivity was estimated by measuring the reflection factor in the coaxial line, using HP 4191A and HP 8510B impedance analysers. The equipment assembled and many times used for dielectric measurements of various ferroelectrics and other crystals at the University of Saarbrücken has been described in [15]. The temperature during the collection of the spectra was stabilised with an accuracy of at least 0.005 K.

3. Result and Discussion

Figure 1 shows the temperature dependence of the real part of the complex electric permittivity measured along the *c*-axis in the frequency range 1 kHz–1 MHz during cooling and heating cycles between 15 and 300 K. It is clearly seen that no dielectric anomaly is visible from the liquid nitrogen temperature down to 15 K. The lower value of the electric permittivity on heating (above the III→II phase transition) in comparison to that observed on cooling is probably connected with the fact that the ferroelastic- ferroelectric phase transition at 134 K is accompanied by a drastic splitting of single crystals parallel to the cleavage plane (001). These measurements showed that no dielectric dispersion at frequencies between 1 kHz and 1 MHz along the crystallographic c-axis of the trigonal room temperature phase in the whole studied temperature range is visible. In our opinion the contribution of the ferroelectric domain walls to the electric permittivity in the vicinity of 134 K is expected to appear below 1 kHz.

Figure 2 shows the real (ε') and imaginary part (ε'') of the complex electric permittivity in the paraelectric (simultaneous paraelastic) phase at 240 and 175 K *vs.* frequency with the Cole-Cole diagrams as an insert. Figure 3 displays ε' and ε'' *vs.* frequency in the ferroelastic phase (II) at 165, 136 and 135 K. The results indicate that the dielectric relaxation in MABA can be well represented by a monodispersive process in a wide temperature region. Figures 2 and 3 indicate that the dielectric relaxation is almost symmetric in nature. Therefore the Cole-Cole relation

$$\varepsilon^* = \varepsilon_\infty + \frac{\varepsilon_s - \varepsilon_\infty}{1 + (jf/f_r)^{1-h}} \tag{1}$$

was used to describe the dielectric response, where f denotes the measuring frequency, f_r the relaxation frequency of the relaxator, ε_s and ε_∞ are limiting values of the permittivity for the low and high frequency region ($\Delta\varepsilon = (\varepsilon_s - \varepsilon_\infty)$ is the amplitude of the relaxator), and the parameter h characterised the distribution of the relaxation time. The solid lines in Figs. 2 and 3 represent the fits to the Cole-Cole function given by (1). Over the paraelectric phase a continuous increase in the relaxation strength $\Delta\varepsilon$ is visible on approaching the 168 K phase transition. At the transition points a step-wise decrease in the $\Delta\varepsilon$ is observed without any important change in the relaxation frequency (f_r). Figure 4 presents the temperature behaviour of the static and high frequency limiting values of ε as fitting parameters. Below 168, over the ferroelastic phase (II), $\Delta\varepsilon$ is practically constant. Fig. 5 presents the log f_r *vs.* T^{-1} plot between 130 and 300 K. It was found that relaxation frequency of the relaxation process follows the Arrhenius relation $f_r = f_0 \exp(-\Delta U/kT)$, giving a quite small value of energy barrier ($U = 0.008$ eV) in the intermediate phase (II). Unexpectedly, in the high temperature phase (I) the estimated energy barrier is practically zero. On the other hand, just below the phase transition at 134 K the energy barrier tends to increase distinctly. However, we have not enough experimental points to estimate it.

It is interesting (see Fig. 4) that ε_∞ in the phases (I) and (II) is still relatively large. Taking into account that the observed dielectric ralaxator revealed its monodispersive nature, an additional dielectric relaxator should appear at frequencies higher than several dozen GHz. The suggested relaxator may be characterised by a dielectric strength ($\Delta\varepsilon$) of the order of 10 units. On the other hand, we can not exclude the possibility that the enhanced electric permittivity ε_∞ may be explained in terms of the "displacive" contribution especially in the vicinity of para-ferroelectric phase transition at 134 K. Such a situation is encountered in the closely related compound $(CH_3NH_3)_3Bi_2Br_9$ (MABB). The low frequency dielectric relaxation in MABB, found around the para-ferroelectric phase transition at 104 K cor-

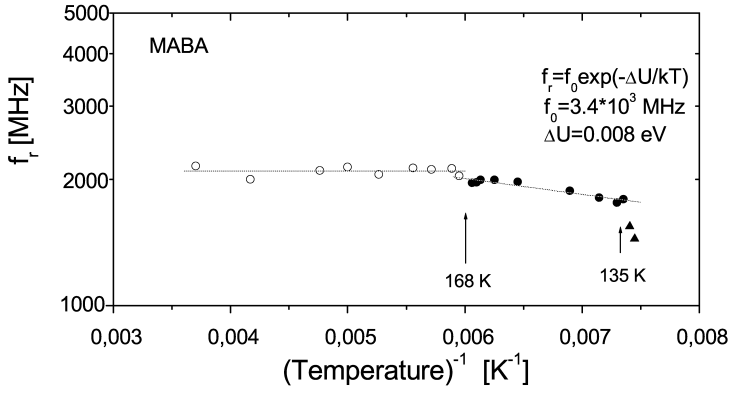

Fig. 5. Arrhenius plot of the relaxation frequency f_r over the paraelastic (I) and ferroelastic phase (II).

responding to the one at 134 K in MABA, did not exhibit Debey-like behaviour, and its mechanism was suggested to be of the displacive type.

The dynamic dielectric behaviour of other methylammonium halogenoantimonate(III) crystals having the same stoichiometry, e.g. $(CH_3NH_3)_3Sb_2I_9$ (MAIA), resembles that found in the title crystal [16]. The single relaxator found in MAIA over a wide temperature region both above and below the 147 K phase transition point showed a comparable relaxation frequency f_r as that estimated for MABA. Similarly as in case of MABA crystals, the dielectric relaxator in MAIA does not show a critical behaviour at 147 K without even noticeable changes in f_r when the phase transition is crossed.

The comparison of dynamic dielectric properties of MABA, MABB and MAIA leads to the conclusion that all methylammonium halogenoantimonate(III) and halogenobismuthate(III) crystals are characterised by similar dynamics of the methylammonium cations. The mechanism of phase transitions seems to be rather complex and the "order-disorder" and "displacive" contribution should be taken into account.

It seems interesting to mention the dielectric properties of closely related ferroelectrics having the same stoichiometry like $[(CH_3)_2NH_2]_3Sb_2Cl_9$ [17], $[(CH_3)_2NH_2]_3Sb_2Br_9$ [18], and $[(CH_3)_3NH]_3Sb_2Cl_9$ [19, 20]. The dynamic dielectric properties of these crystals were determined by the presence of two independent relaxators. The low frequency relaxator revealed a critical slowing down close to T_c, whereas the high frequency one was only thermally activated, showing only a subtle change in the relaxation frequency at T_c. The latter relaxator possesses the same features as those found in a case of the high frequency relaxator MABA crystal.

4. Conclusion

(i) The dielectric properties of MABA in the high-frequency range from 1 MHz to 3 GHz are described by the presence of a single Cole-Cole type relaxator in the phases (I) and (II).

(ii) The relaxation frequency of the dielectric relaxator fulfils the Arrhenius relation with a relatively small activation energy, which changes insignificantly on passing through the (I→II) phase transition at 168 K.

(iii) The amplitude of the relaxator ($\Delta\varepsilon$) changes stepwise at the phase transition points (at 168 and 134 K) as expected from the low-frequency dielectric measurements.

(iv) Both the "order-disorder" and "displacive" contributions are suggested to appear in the phase transition mechanism at 134 K.

[1] R. Jakubas and L. Sobczyk, Phase Transitions **20**, 163 (1990).
[2] M. Bujpk and J. Zaleski, Crystal Eng. **4**, 241 (2001).
[3] V. Varma, R. Bhattacharjee, H. N. Vasan, and C. N. R. Rao, Spectrochim. Acta **48A**, 1631 (1992).
[4] H. Ishihara, K. Watanabe, A. Iwata, K. Yamada, Y. Kinoshita, T. Okuda, V. G. Krishnan, S. Dou, and Al. Weiss, Z. Naturforsch. **47a**, 65 (1992).
[5] M. Iwata, M. Eguchi, Y. Ishibashi, S. Sasaki, H. Shimizu, T. Kawai, and S. Shimanuki, J. Phys. Soc. Japan **62**, 3315 (1993).
[6] S. Ishimaru, K. Suzuki, and R. Ikeda, J. Phys. Soc. Japan **64**, 1754 (1995).
[7] T. Kawai, A. Ishii, T. Kitamura, S. Shimanuki, M. Iwata, and Y. Ishibashi, J. Phys. Soc. Japan **65**, 1464 (1996).

[8] K. Gesi, M. Iwata, and Y. Ishibashi, J. Phys. Soc. Japan **65**, 14 (1996).
[9] T. Kawai, E. Takao, S. Shimanuki, M. Iwata, A. Miyashita, and Y. Ishibashi, J. Phys. Soc. Japan **68**, 2848 (1999).
[10] M. Iwata, A. Miyashita, H. Orihara, Y. Ishibashi, M. H. Kuok, Z. L. Rang, and S. C. Ng, Ferroelectrics **229**, 233 (1999).
[11] M. Iwata and Y. Ishibashi, Ferroelectrics **135**, 283 (1992).
[12] Y. Iwata, N. Koyano, M. Machida, M. Iwata, and Y. Ishibashi, Ferroelectrics **237**, 229 (2000)
[13] M. H.,Kuok, S. G. Ng, L. S. Tan, Z. L. Rang, M. Iwata, and Y. Ishibashi, Solid State Commun. **108**, 159 (1998).
[14] W. Medycki, Solid State NMR **14**, 137 (1999).
[15] Cz. Pawlaczyk, K. Planta, Ch. Bruch, J. Stephan, and H.-G. Unruh, J. Phys.: Condens. Matter. **4**, 2687 (1992).
[16] Cz. Pawlaczyk, R. Jakubas, and H.-G. Unruh, Solid State Commun. **108**, 247 (1998).
[17] G. Bator and R. Jakubas, Phys. Status Solidi **A 147**, 591 (1995).
[18] J. Zaleski, Cz. Pawlaczyk, R. Jakubas, and H.-G. Unruh, J. Phys.: Condens. Matter **12**, 7509 (2000).
[19] G. Bator, R. Jakubas, J. Zaleski, and J. Mróz, J. Appl. Phys. **88**, 1015 (2000).
[20] R. Sobiestianskas, Z. Czapla, and J. Grigas, Phys. Status Solidi **A 130**, K69 (1992).